

The DFT Study of Oxygen Adsorption on Pristine and As-Doped of the (4, 4) Armchair Models BNNTs

M. Rezaei-Sameti ^{1*}and F.Khaje Joushaghani

¹Department of Physical Chemistry, Faculty of Science, Malayer University, Malayer, 65174, Iran

Abstract

In this work, the effects of As-doped on the adsorption of oxygen gas on the outer and inner surface of boron nitride nanotube (BNNTs) is investigated. The structural parameters, quantum properties involving: bond length, bond angle, HOMO-LUMO orbital, gap energy, electron affinity, electronegativity, chemical potential, global hardness, global softness and NMR parameters of BNNTs are calculated at different configurations of O₂adsorption on the outer and inner surface of BNNTs by performing density functional theory (DFT) using Gaussian 03 package of program. Our results reveal that the adsorption energy of all models is exothermic and the E_{ads} value in (A and B) undoped models of BNNTs is larger than those of the other models. The results show that As-doped impurities and O₂ adsorption decrease the adsorption energy of O₂gas on the surface of BNNTs and the gap energy between HOMO-LUMO orbital and increase the conductivity of nanotube.

Keywords: BNNTs, Adsorption O₂, As-doped, DFT, NMR

1. Introduction

Soon after the theoretical and experimental approach on BNNTs [1, 2], Considerable theoretical and experimental efforts have been devoted to investigate the electrical and structural properties and applications of (BNNTs) [3–8]. The structural properties of BNNTs are similar CNTs, while their electronic properties are quite different from CNTs,

however they exhibit only semiconducting properties independent of their chirality and diameter with wide band gaps ranging from 4 to 5.5 eV. Like diamond, boron nitride acts as an electrical insulator, but it is an excellent conductor of heat [9–15]. Recent experimental and theoretical studies have a strong interest on the phenomenology of gas molecules such as O₂, NO₂, NH₃, and many other gases, at ambient temperature on nanotube [15–20]. In the last years, several theoretical studies have been performed to study the adsorption of O₂ on single-walled carbon nanotubes (SWNT)

*Correspondig Author

E-mail address: mrsameti@gmail.com
mrsameti@malayeru.ac.ir

using density functional theory (DFT) [21-26]. Recent researches show that interaction of oxygen with nanotubes have always been an interesting and fascinating subject for the scientific community for both fundamental and practical reasons, as well as for the possible applications and chemical manufacturing processes in nano device technologies and in chemical sensors[27-34]. Following our previous research on the electrical structural and NMR parameters SiC-doped AlPNTs, Ga, Al, N, Ge, As doped BPNTs [35-38], in the present work, we investigate the sensitivity of BNNTs toward O₂ molecules at different positions of outside and inside of BNNTs and the effect of As doped on the adsorption. The chemical shielding (CS) tensors originating at the sites of half-spin nuclei, structural properties and quantum parameters involving: HOMO-LUMO orbital, gap energy, other quantum molecular descriptors at different situation of O₂ adsorption inside and outside of BNNTs are investigated by performing density functional theory (DFT) using Gaussian 03 package of program.

2. Computational methods

The structural and electrical properties of (4, 4) armchair models of undoped and As-doped of BNNTs (see Figs.1-2) with adsorption of O₂ on the surface of nanotubes are investigated by density function theory at B3LYP level of theory using the Gaussian 03 set of programs [39-40]. After optimizing all consider structures of nanotubes, the chemical shielding (CS) tensors at the sites of ¹¹B, ¹⁴N nuclei based on the gauge included atomic orbital (GIAO) approach and same level of theory [41]. The calculated CS tensors in principal axes system (PAS) ($\sigma_3 > \sigma_2 > \sigma_1$) are converted to measurable NMR parameters,

chemical shielding isotropic (CSI) and chemical shielding anisotropic (CSA) by using equations (1) and (2), respectively [35-38].

$$CSI(ppm) = \frac{1}{3}(\sigma_1 + \sigma_2 + \sigma_3) \quad (1)$$

$$CSA(ppm) = \sigma_3 - (\sigma_1 + \sigma_2)/2 \quad (2)$$

Adsorption energy (E_{ads}) of oxygen gas on the surface of pristine and As-doped BNNTs was calculated as follow:

$$E_{ads} = E_{BNNTs-O_2} - (E_{BNNTs} + E_{O_2}) + BSSE \quad (3)$$

Where E_{BNNTs-O₂} was obtained from the scan of the potential energy of the BNNTs-O₂, E_{BNNTs} is the energy of the optimized BNNTs structure, and E_{O₂} is the energy of an optimized O₂ and BSSE is base set superposition errors. The quantum molecular descriptors: electronic chemical potential (μ), global hardness (η), electrophilicity index (ω), energy gap, global softness (S), electronegativity (χ) and maximum amount of electronic charge, ΔN , of the nanotubes [42-45] were calculated as the following equitations indicate:

$$\mu = -(I + A)/2 \quad (4)$$

$$\mu = -x \quad (5)$$

$$\omega = \mu^2 / 2\eta \quad (6)$$

$$\eta = (I - A)/2 \quad (7)$$

$$S = 1/2\eta \quad (8)$$

$$E_{gap} = E_{LUMO} - E_{HOMO} \quad (9)$$

$$\Delta N = \frac{-\mu}{\eta} \quad (10)$$

Where I(-E_{HOMO}) is the ionization potential and A (-E_{LUMO}) the electron affinity of the molecule. The electrophilicity index is a measure of the

electrophilic power of a molecule.

3. Results and discussion

3.1 Structural Properties

In this work, we begin our study with oxygen gas adsorption on the outer and inner surface of pristine and As-doped (4, 4)

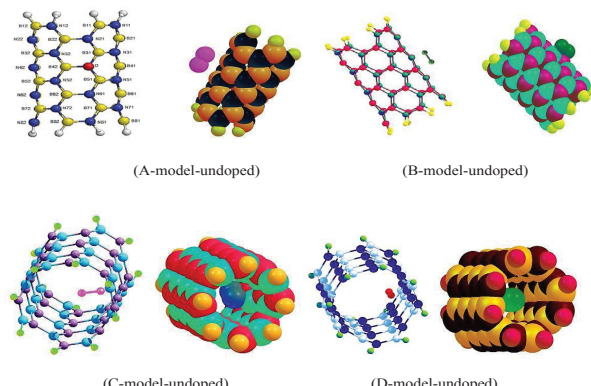


Fig. 1 2D views of O_2 adsorption on the undoped of (4, 4) armchair model of BNNTs;
Model A shows the vertical adsorption of O_2 gas on the outer surface of nanotube.
Model B shows the vertical adsorption of O_2 gas on the inner surface of nanotube.
Model C shows the parallel adsorption of O_2 gas on the outer surface of nanotube.
Model D shows the parallel adsorption of O_2 gas on the inner surface of nanotube

armchair BNNTs with the diameters 5.4 Å. For this aim, we consider four models (A-D) for adsorption of O_2 gas on the surface of nanotube. Model A shows the vertical adsorption of O_2 gas on the outer surface of nanotube, Model B indicates the vertical adsorption of O_2 gas on the inner surface of nanotube, Model C shows the parallel adsorption of O_2 gas on the outer surface of nanotube, and Model D demonstrates the parallel adsorption of O_2 gas on the inner surface of nanotube (See Figures 1-2). The structural properties such as bond length and

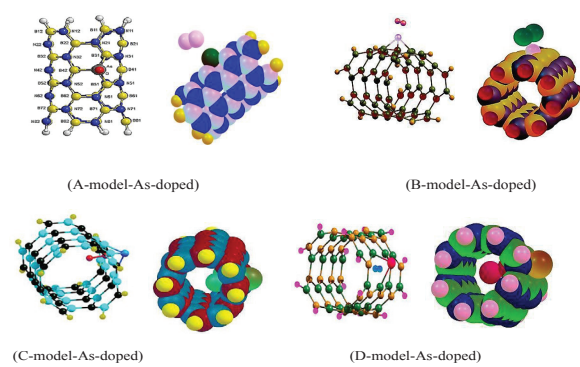


Fig. 2. 2D views of O_2 adsorption on the As-doped of (4, 4) armchair model of BNNTs; For (A-D) models (see Fig. 1).

Table 1. Structures parameters of O_2 adsorption on undoped and As-doped of (4, 4) armchair models of BNNTs, first value for undoped and second value for As-doped of (A-D)models of adsorption.see Fig. 1,2)

Bondlength (Å)	Unadsobed	Model (A)	Model (B)	Model (C)	Model (D)
$B_{42}-N_{41}/As$	1.46 [2.01]	1.45[2.01]	1.53 [2.01]	1.46[2.17]	1.52[2.15]
$B_{31}-N_{41}/As$	1.46[1.98]	1.46[1.98]	1.52[2.02]	1.46[2.14]	1.52[1.98]
$B_{51}-N_{41}/As$	1.46[1.97]	1.45[1.97]	1.64[1.99]	1.45[3.13]	1.60[2.05]
$B_{42}-N_{32}$	1.46 [1.45]	1.45[1.44]	1.43 [1.44]	1.45 [1.45]	1.43 [1.47]
$B_{31}-N_{21}$	1.46 [1.46]	1.46[1.46]	1.45 [1.46]	1.46 [1.54]	1.44 [1.47]
$B_{42}-N_{52}$	1.46 [1.45]	1.45[1.44]	1.42 [1.44]	1.45 [1.45]	1.42 [1.45]
$B_{51}-N_{61}$	1.46 [1.45]	1.45[1.45]	1.51 [1.44]	1.45 [1.42]	1.47 [1.49]
$B_{31}-N_{31}$	1.46 [1.44]	1.45[1.44]	1.41 [1.44]	1.45 [1.46]	1.42 [1.43]
$B_{51}-N_{51}$	1.46 [1.44]	1.45[1.44]	1.50 [1.44]	1.45 [1.41]	1.48 [1.49]
Bond angle(°)					
$<B_{31}-N_{41}/As-B_{42}$	115[88]	115[88]	110[90]	116[78]	123[96]
$<N_{41}/As-B_{42}-N_{32}$	118[118]	119[118]	116[117]	119[107]	113[112]
$<N_{21}-B_{31}-N_{41}/As$	120[114]	120[114]	117[114]	120[68]	116[110]
$<N_{41}/As-B_{42}-N_{52}$	119[119]	120[119]	119[117]	120[133]	117[109]
$<N_{61}-B_{51}-N_{41}/As$	120[114]	119[114]	111[113]	118[96]	115[106]
$<B_{51}-N_{41}/As-B_{42}$	116[87]	119[88]	119[91]	117[63]	115[89]
$<B_{51}-N_{41}/As-B_{31}$	120[95]	119[95]	115[98]	119[49]	122[98]
$<N_{41}/As-B_{31}-N_{31}$	118[124]	116[124]	119[122]	119[147]	114[118]
$<N_{51}-B_{51}-N_{41}/As$	119[125]	115[125]	130[124]	120[120]	113[116]

bond angel of pristine and four adsorption models are given in Table 1. Comparing results reveal that the bond length of B_{42} - N_{41} , B_{31} - N_{41} , B_{51} - N_{41} of (B, D) undoped models increase from 1.46 to 1.52, 1.52, and 1.60 Å respectively. On the other hand, the adsorption of O_2 on the B model caused that the bond length of B_{51} - N_{61} , B_{51} - N_{51} increase from 1.46 to 1.51 and 1.50 Å respectively, due to interaction π electron of O_2 gas with nanotube. And also the s-character of the hybridized orbitals decrease which leads to an increase in the interaction of nanotube orbitals with the O_2 orbitals. With doping As in the B41 nuclei of nanotube, the B_{42} - N_{41} , B_{31} - N_{41} , B_{51} - N_{41} bond length increase from 1.46 to 2.01, 1.98 and 1.97 Å respectively, because the radius of As is more than B atoms. The adsorption of O_2 gas increases significantly the bond length of neighbourhood As-doped. The increase of bond length on the C model is larger than other models. The bond angles of neighbourhood As-doped of BNNTs in all models decrease from pristine models due to more radius of As respect B atoms. The bond angle of $\angle B_{31}-N_{41}/$

$As-B_{42}$ of B model of undoped nanotube decrease from 115 to 110° and at Dmodel of undoped this bond angle increase to 123°. The bond angles $\angle B_{31}-N_{41}/As-B_{42}$, $\angle N_{21}-B_{31}-N_{41}/As$, $\angle B_{51}-N_{41}/As-B_{42}$ and $\angle B_{51}-N_{41}/As-B_{31}$ of Cmodel decrease from original values in As-doped of nanotube and $\angle N_{41}/As-B_{31}-N_{31}$ of this model increase significantly to 147° in As doped.

The results of adsorption energies between nanotube and O_2 gas calculated on Eqs. 3 are given in Table 2. The results show that the adsorption energy of all models is exothermic and at the (A and B) models the adsorption energy values are more than other models. On the other hand with doping As, the adsorption energy decreases largely from undoped model, this result demonstrates that As-doped is not favorable for O_2 adsorption in all models. Base set superposition error for all models is 0.01 eV.

3.2 Electronic and quantum properties

Table 2 presents the results for the HOMO, LUMO, gapenergies, and quantum

Table 2. Quantum parameters of O_2 adsoption on pristine and As-doped of (4, 4) armchair models of BNNTs.

BNNT(4,4)											
O_2	pristine	As-doped	Model (A)		Model (B)		Model (C)		Model (D)		
			Un doped	As Doped	Un doped	As Doped	Un doped	As Doped	Un doped	As Doped	
E(ads)/kcal/mol	-	-	-	-19.45	-0.27	-19.37	-0.13	-18.87	-0.12	-17.41	-1.36
E(Bsse)/ev	-	-	-	0.01	0.012	0.01	0.03	0.01	0.02	0.01	0.02
E(HOMO)/ev	-6.81	-6.32	-6.38	-6.23	-5.04	-6.29	-5.29	-6.47	-6.06	-6.32	-6.16
E(LUMO)/ev	-4.77	-0.11	-0.75	-4.18	-3.05	-1.68	-1.96	-4.79	-2.01	-1.95	-3.87
E(gap)/ev	2.04	6.21	5.63	2.05	1.99	4.61	3.33	1.68	4.05	4.37	2.29
η/ev	1.02	3.11	2.82	1.03	0.99	2.31	1.67	0.84	2.02	2.19	1.14
$S/(ev)^{-1}$	0.49	0.16	0.18	0.48	0.51	0.22	0.30	0.59	0.25	0.23	0.44
μ/ev	-5.79	-3.22	-3.57	-5.21	-4.05	-3.99	-3.63	-5.63	-4.03	-4.14	-5.01
χ/ev	5.79	3.22	3.57	5.21	4.05	3.99	3.63	5.63	4.03	4.14	5.01
ω/ev	16.43	1.67	2.26	13.18	8.28	3.45	3.94	18.87	4.02	3.91	11.01
ΔN	5.68	1.03	1.27	5.06	4.09	1.73	2.17	6.70	1.99	1.89	4.39

parameters obtained by the DFT calculations and Eqs. (4-9). Calculated gap energies for the isolated nanotubes are 6.21 eV in pristine and 5.43 eV in As-doped models. With adsorbing O₂ gas on the outer surface of the nanotube, the gap energy between HOMO-LUMO orbital decrease from original values due to donor electron effects of O₂ gas. This lowering of gap energy with O₂ adsorption may be able to increase the reactivity of the O₂/BNNTs complex, and shows charge transfer to take place between the π electron of O₂ and BNNTs sidewall.

The electronic chemical potential (μ), global hardness (η) of O₂ adsorption on surface of BNNTs is presented in Table 2. The results show that, the chemical potential and global hardness decrease with decrease in gap energy. The results also show that the chemical potential and global hardness in C undoped model of nanotube is lower than other models. Therefore, we can predict that adsorbing O₂ decreases the stabilities of pristine nanotube. The comparison of electronegativity (χ) of the nanotubes reveals that with adsorbing O₂ the electronegativity increases from pristine models. The electronegativity of undoped C model is larger than other models and the electronegativity of As-doped B model is lower than other models. By bringing the O₂ gas and nanotubes together, electrons will flow from that of lower electronegativity atoms to that of higher electronegative atom. Therefore, the difference in electronegativity drives the electron transfer. As a result, electrons will flow from a definite occupied orbital in a nanotube and will go into a definite empty orbital in an O₂ molecule. The overlap between the exchanging orbitals will be critical in determining the energy changes. In addition, the values for gap energy and hardness for O₂ molecule is smaller than the nanotube; these

results lead that O₂ molecule having higher polarizability than the nanotubes. The amount of charge transfer (ΔN) between the O₂ molecule and (A-D) models of adsorption, as calculated using the Eq. (10) and given in Table 2. In all models, ΔN values are positive and indicate that O₂ molecule act as an electron acceptor. The ΔN values of undoped C model are significantly larger than other models and therefore in this model, the charge transfer from nanotube to O₂ gas is larger than other model.

3.3 NMR parameters

The NMR (CSI and CSA) parameters of ¹¹B and ¹⁴N nuclei for the pristine, As-doped of (4, 4) armchair BNNTs in present of O₂-adsorption ((A-D) models Fig. 1, 2) are calculated by Eqs (1, 2) and given in Tables (3-6). A look at results of A model (Table 3) show that with doping As atom the CSI values of ¹¹B nuclei at the sites B31, B42, B51 decrease significantly from 82, 80 and 81 ppm to 61, 71, and 63 respectively. On the otherwise, the CSA values of ¹¹B nuclei at the layers 1, 3, 5, 7 increases from undoped model and on the other layers increase. The direction of changes for isotropic and anisotropic chemical shielding because of difference in physical concept of these parameters is different. The CSI values of ¹⁴N nuclei at the N21, N32, and N61 with doping As decrease significantly from undoped model, due to donor electron effect of As-doped. The CSA values of ¹⁴N nuclei at the layers 1, 3, 5, 7 decreases from undoped model and the other layers increase.

In the B model, the CSI values at B31, B42, B51, B52 sites decrease largely from original values. The CSA values of ¹¹B nuclei at the layers 1, 3, 5, 7 are decreased from undoped model and the other layers increase, the similar results are shown for A model. The CSI values

Table 3. NMR parametres of O₂ adsorption on undoped and As-doped of (4, 4) armchair BNNTs, (**A**) model of Fig.1.

B-11 nuclei	CSI (ppm)		CSA (ppm)		N-14 nuclei	CSI (ppm)		CSA (ppm)	
	Undoped	Doped	Undoped	Doped		Undoped	Doped	Undoped	Doped
B ₁₁	80	84	18	37	N ₁₁	146	147	80	65
B ₁₂	80	80	19	34	N ₁₂	146	143	75	68
B ₁₃	80	80	20	31	N ₁₃	146	146	80	69
B ₁₄	80	80	19	32	N ₁₄	146	146	82	69
B ₂₁	84	86	34	28	N ₂₁	137	113	132	157
B ₂₂	84	82	33	27	N ₂₂	136	136	135	167
B ₂₃	84	84	34	30	N ₂₃	136	135	135	162
B ₂₄	84	84	34	30	N ₂₄	136	139	135	169
B ₃₁	82	82	15	29	N ₃₁	134	120	139	106
B ₃₂	82	81	15	24	N ₃₂	134	134	136	103
B ₃₃	82	83	15	26	N ₃₃	134	135	135	86
B ₃₄	82	83	35	26	N ₃₄ /As	124	-	164	-
B ₄₁	80	71	36	24	N ₄₁	140	138	138	167
B ₄₂	82	81	34	31	N ₄₂	140	140	137	162
B ₄₃	82	82	34	29	N ₄₃	140	142	138	163
B ₄₄	81	63	19	26	N ₄₄	141	126	141	113
B ₅₁	81	83	16	25	N ₅₁	139	125	138	67
B ₅₂	82	81	15	23	N ₅₂	140	139	137	105
B ₅₃	82	83	15	26	N ₅₃	140	141	136	88
B ₅₄	82	83	35	31	N ₅₄	117	112	165	152
B ₆₁	81	80	38	26	N ₆₁	134	135	137	164
B ₆₂	82	82	35	32	N ₆₂	134	134	137	161
B ₆₃	82	82	35	30	N ₆₃	134	136	137	169
B ₆₄	84	86	17	28	N ₆₄	135	137	148	100
B ₇₁	84	84	17	27	N ₇₁	136	133	146	98
B ₇₂	84	84	17	26	N ₇₂	136	136	145	107
B ₇₃	84	83	17	26	N ₇₃	136	135	144	103
B ₇₄	84	83	17	26	N ₇₄	147	147	121	123
B ₈₁	80	80	53	49	N ₈₁	146	145	122	126
B ₈₂	80	80	53	50	N ₈₂	146	146	122	125
B ₈₃	80	80	53	49	N ₈₃	146	146	123	125
B ₈₄	80	80	53	50	N ₈₄	146	146	123	125
As					As	1815			546

Table 4 NMR parametres of O₂ adsorption on undoped and As-doped of (4, 4) armchair BNNTs, (**B**) model of Fig.1.

B-11 nuclei	CSI (ppm)		CSA (ppm)		N-14 nuclei	CSI (ppm)		CSA (ppm)	
	Undoped	Doped	Undoped	Doped		Undoped	Doped	Undoped	Doped
B ₁₁	80	84	45	37	N ₁₁	143	146	91	63
B ₁₂	80	80	44	35	N ₁₂	145	142	97	58
B ₁₃	80	80	46	30	N ₁₃	147	147	87	68
B ₁₄	80	80	43	33	N ₁₄	146	146	95	42
B ₂₁	84	86	22	27	N ₂₁	137	114	181	143
B ₂₂	85	83	18	27	N ₂₂	139	136	171	170
B ₂₃	84	84	22	31	N ₂₃	136	135	184	161
B ₂₄	84	84	21	29	N ₂₄	135	139	180	171
B ₃₁	82	70	33	7	N ₃₁	129	123	67	118
B ₃₂	80	82	31	26	N ₃₂	127	113	68	59
B ₃₃	82	81	33	24	N ₃₃	133	133	54	105
B ₃₄	81	83	32	27	N ₃₄ /As	135	135	52	81
B ₄₁	85	85	17	25	N ₄₁	145	-	172	-
B ₄₂	81	72	17	21	N ₄₂	125	138	143	169
B ₄₃	81	81	23	32	N ₄₃	138	140	179	161
B ₄₄	81	82	20	28	N ₄₄	140	143	173	164
B ₅₁	82	63	32	16	N ₅₁	147	119	64	126
B ₅₂	104	83	6	27	N ₅₂	133	124	63	68
B ₅₃	81	81	32	23	N ₅₃	139	139	57	107
B ₅₄	81	83	31	27	N ₅₄	141	141	51	84
B ₆₁	83	84	21	30	N ₆₁	138	138	175	148
B ₆₂	84	82	23	26	N ₆₂	137	135	149	165
B ₆₃	82	82	24	32	N ₆₃	135	134	176	161
B ₆₄	82	82	21	29	N ₆₄	134	136	173	170
B ₇₁	84	87	33	29	N ₇₁	135	137	53	98
B ₇₂	83	85	33	28	N ₇₂	136	133	42	95
B ₇₃	84	84	32	25	N ₇₃	136	136	58	108
B ₇₄	83	84	33	26	N ₇₄	136	135	47	101
B ₈₁	80	80	42	49	N ₈₁	148	148	117	123
B ₈₂	80	80	41	51	N ₈₂	143	145	120	127
B ₈₃	80	80	41	49	N ₈₃	145	146	118	125
B ₈₄	80	80	40	50	N ₈₄	146	146	117	126
As					As	1675			549

Table 5 NMR parametres of O₂ adsorption on undoped and As-doped of (4, 4) armchair BNNTs, (**C**) model of Fig.1.

B-11 nuclei	CSI (ppm)		CSA (ppm)		N-14 nuclei	CSI (ppm)		CSA (ppm)	
	Undoped	Doped	Undoped	Doped		Undoped	Doped	Undoped	Doped
B ₁₁	81	77	32	16	N ₁₁	146	131	67	77
B ₁₂	80	79	29	14	N ₁₂	146	146	61	87
B ₁₃	81	80	32	18	N ₁₃	146	146	67	74
B ₁₄	81	81	29	22	N ₁₄	146	145	62	69
B ₂₁	84	84	29	30	N ₂₁	136	136	168	47
B ₂₂	85	80	30	30	N ₂₂	136	131	160	140
B ₂₃	84	83	29	35	N ₂₃	136	137	168	134
B ₂₄	85	84	30	35	N ₂₄	136	135	160	138
B ₃₁	83	106	26	19	N ₃₁	135	135	92	96
B ₃₂	81	81	22	19	N ₃₂	135	135	110	86
B ₃₃	83	82	26	16	N ₃₃	135	135	92	130
B ₃₄	81	80	22	13	N ₃₄ /As	135	135	110	141
B ₄₁	79	81	31	31	N ₄₁ /As	114	-	206	-
B ₄₂	81	74	34	15	N ₄₂	135	143	163	151
B ₄₃	79	81	31	33	N ₄₃	114	143	207	134
B ₄₄	81	81	34	35	N ₄₄	135	140	167	140
B ₅₁	79	88	35	13	N ₅₁	139	147	98	97
B ₅₂	77	80	26	19	N ₅₂	138	138	124	101
B ₅₃	79	81	35	36	N ₅₃	140	143	98	132
B ₅₄	77	79	27	12	N ₅₄	138	139	124	146
B ₆₁	79	81	32	32	N ₆₁	105	145	212	108
B ₆₂	80	78	35	37	N ₆₂	128	133	165	146
B ₆₃	80	82	32	33	N ₆₃	104	135	213	128
B ₆₄	80	81	35	36	N ₆₄	128	131	165	135
B ₇₁	85	84	27	17	N ₇₁	137	138	95	130
B ₇₂	83	84	23	18	N ₇₂	134	131	122	154
B ₇₃	85	84	27	15	N ₇₃	137	137	95	140
B ₇₄	83	83	23	17	N ₇₄	134	134	122	154
B ₈₁	81	81	48	51	N ₈₁	146	147	128	115
B ₈₂	80	80	50	49	N ₈₂	145	148	122	122
B ₈₃	81	80	48	52	N ₈₃	146	146	128	118
B ₈₄	80	79	50	54	N ₈₄	145	145	122	122
As					As		1042		1127

Table 6 NMR parametres of O₂ adsorption on undoped and As-doped of (4, 4) armchair BNNTs, (**D**) model of Fig.1.

B-11 nuclei	CSI (ppm)		CSA (ppm)		N-14 nuclei	CSI (ppm)		CSA (ppm)	
	Undoped	Doped	Undoped	Doped		Undoped	Doped	Undoped	Doped
B ₁₁	80	84	42	23	N ₁₁	143	147	90	67
B ₁₂	80	79	38	21	N ₁₂	142	138	75	100
B ₁₃	80	81	42	16	N ₁₃	147	147	89	81
B ₁₄	80	79	38	23	N ₁₄	145	145	70	90
B ₂₁	83	85	26	32	N ₂₁	137	121	177	79
B ₂₂	83	83	27	34	N ₂₂	135	135	177	124
B ₂₃	84	85	21	34	N ₂₃	135	136	182	117
B ₂₄	84	83	26	35	N ₂₄	136	138	175	110
B ₃₁	84	70	28	11	N ₃₁	133	125	64	115
B ₃₂	79	78	30	17	N ₃₂	129	146	95	75
B ₃₃	82	82	31	12	N ₃₃	135	136	47	140
B ₃₄	81	82	29	8	N ₃₄ /	134	134	75	155
B ₄₁	79	80	22	26	N ₄₁ /	99	-	197	-
B ₄₂	79	89	28	28	As	139	137	169	125
B ₄₃	81	81	20	35	N ₄₃	141	143	176	122
B ₄₄	81	82	27	36	N ₄₄	133	135	173	115
B ₅₁	106	121	22	24	N ₅₁	169	172	30	132
B ₅₂	79	78	29	12	N ₅₂	134	140	103	116
B ₅₃	82	82	30	12	N ₅₃	142	142	51	142
B ₅₄	80	80	28	9	N ₅₄	140	141	79	155
B ₆₁	79	81	23	34	N ₆₁	140	136	159	97
B ₆₂	78	80	30	36	N ₆₂	133	130	173	121
B ₆₃	81	82	21	34	N ₆₃	136	137	174	122
B ₆₄	81	82	27	36	N ₆₄	127	126	173	112
B ₇₁	85	87	28	18	N ₇₁	135	138	22	137
B ₇₂	83	83	30	9	N ₇₂	131	128	85	172
B ₇₃	84	84	31	15	N ₇₃	137	138	55	146
B ₇₄	83	83	30	9	N ₇₄	135	135	81	170
B ₈₁	80	80	41	53	N ₈₁	145	147	121	123
B ₈₂	80	80	46	53	N ₈₂	146	145	119	116
B ₈₃	80	80	41	52	N ₈₃	147	147	121	119
B ₈₄	80	80	46	53	N ₈₄	147	146	116	113
As					As	75		1229	

of ^{14}N nuclei at the N21, N32, N51 and N61 sites of As-doped decrease significantly from undoped model. In addition, the CSA values of ^{14}N nuclei at the layers 1, 4, 6 decrease and other layers increase. The results of Table 5 for C models reveal that the CSI values of ^{11}B

nuclei with As-doped at the B42 site decrease largely from 81 to 74 ppm and at sites B31 and B52 increase from 83, 77 ppm to 106 and 80 respectively. The CSA value of ^{11}B nuclei at the layers 1, 3, 7 decreases from undoped model and the other sites increase. The CSI values of

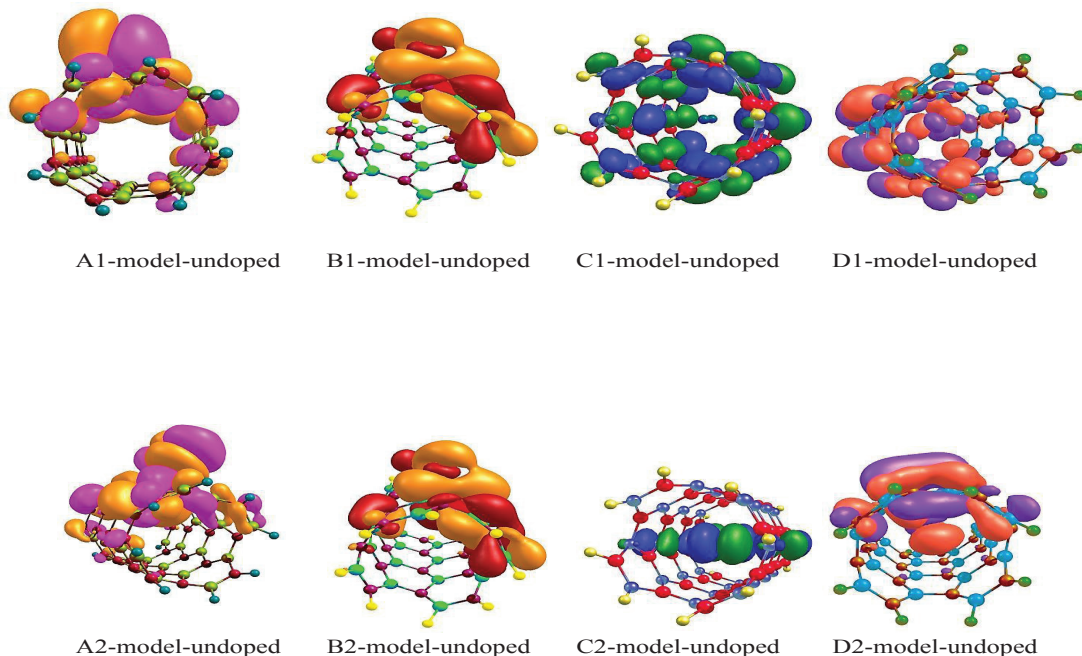


Fig. 3 Comparisons the HOMO-LUMO structures of O_2 adsorption on the undoped of (4,4) armchair model of BNNTs, index (1) used for HOMO and index (2) for LUMO (A-D) models (see Fig.1).

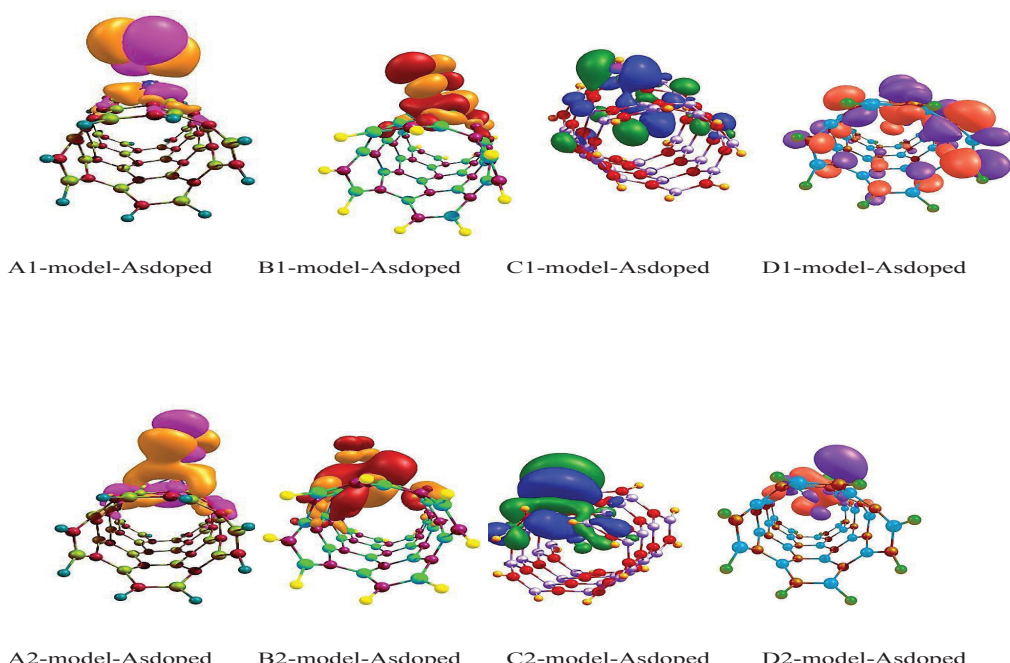


Fig. 4 Comparisons the HOMO-LUMO structures of O_2 adsorption on the As-doped of (4,4) armchair model of BNNTs, index (1) used for HOMO and index (2) for LUMO (A-D)models (see Fig.2).

¹⁴N nuclei at the N21, N31, N43, N52, N61, and N63 sites increase from undoped model. The CSA values of ¹⁴N nuclei at the layers 2, 4, 6, 8decreases from undoped model and the other layers increase.The calculated results of D model (Table 6) show that the CSI values of ¹¹B nuclei with As-doped at B42 and B51 sites increase from 79, 106 ppm to 89, 121ppm, and at site B31 decrease from 84 to 76 ppm. CSA values of ¹¹B nuclei at odd layers decrease and even layers increase from undoped models. On the other hand, the CSI values of ¹⁴N nuclei at the sites N21, N31 and N61 decrease and at sites N32, N51 and N52 increase from undoped model. In addition, the CSA values of ¹⁴N nuclei at even layers decrease and at layers 3, 5, 7 increase significantly from undoped models.The comparison results show that the CSI and CSA values depended on either As-doped or configurations of O₂ adsorption.

4. Conclusions

In this research we studied the adsorptions of O₂gas on four models of the outer and inner surface of pristine and As-doped (4, 4) armchair BNNTs by means of density functional theory (DFT) calculations. The results reveal that adsorption energy of undoped of nanotube in four models are exothermic and at the (A and B)models are more than other models, so the adsorption O₂ on surface of these models are favorable than other models. With doping As in all models the adsorption energy is decrease. The gap energy between LUMO-MOMO orbital with adsorbing O₂ gas on the surface of nanotube decrease and so the conductivity properties of nanotube are increase. The gap energy of undoped C model is lower than other models. The comparing results of quantum properties reveal that the global hardness, electronic chemical potential and stability of

nanotube are decrease and so the reactivity of the O₂ adsorbed is increase.The comparison results of NMR parameters show that the CSI and CSA values depended on either As-doped or configurations of O₂ adsorption.

Acknowledgment

The authors thank the centre of computational nano of Malayer University for supporting this research.

References

- [1] X. Blase, A. Rubio, S.G. Louie, M.L. Cohen,Euro. phys. Lett. 28(1994) 335.
- [2] N.G. Chopra, R.J. Luyken, K. Cherrey, V.H. Crespi, M.L. Cohen, S.G. Louie, A. Zettl,Science.269(1995) 966.
- [3]Q. Dong, X. M. Li, W. Q. Tian, X. R. Huang, C. C. Sun,J. Mol. Stru.(THEOCHEM) 948 (2010)83.
- [4]E. Bengu, L.D. MarksPhys. Rev. Lett. 86(2001)2385.
- [5] K.B. Shelimov, M. Moskovits,Chem. Mater. 12(2000) 250.
- [6] R.J. Baierle, P. Piquini, T.M. Schmidt, S.J. Fazzio,J. Phys. Chem. B. 110 (2006) 21184.
- [7] H. Chen, Y. Chen, C.P. Li, H. Zhang, J.S. Williams, Y. Liu, Z. Liu, S.P. Ringer,Adv.Mater. 19(2007) 1845.
- [8] D. Golberg, Y. Bando, M. Eremets, K. Takemura ,K. Kurashima , H. Yusa,Appl. Phys. Lett.69(1996) 2045.
- [9] H. Chen, H. Zhang, L. Fu, Y. Chen, J.S. Williams, C. Yu, D. Yu,Appl. Phys. Lett. 92 (2008) 243105.
- [10] S.A. Shevlin, Z.X. Guo, Phys. Rev. B. 76 (2007) 024104.
- [11] A. Ahmadi, J. Beheshtian. N. L. Hadipour, (2011). Struct.Chem. 22,183.
- [12] A. Ahmadi, M. Kamfirooz, J. Beheshtian, N. L. Hadipour,Struct Chem. 22(2011) 1261.
- [13] S.F. Wang, J.M. Zhang, K.W. Xu,Physica B. 405(2010) 1035.
- [14] R. Chegel, S. Behzad, Solid State Comm. 151(2011) 259.
- [15] H. Roohi, S. Bagheri,J. Mol. Stru. (THEOCHEM) 856(2008) 46.
- [16]J. Beheshtian, H. Soleymanabadi ,M. Kamfirooz ,A. Ahmadi,J. Mol. Model.18(2011) 2343.
- [17] V. Nirmala, P. Kolandaivel,J. Mo. Struct. (THEOCHEM).817(2007) 137.
- [18] M. Mirzaei, Z.Phys. Chem. 223(2009) 815.
- [19] L. Chen, G.Q. Zhou, C. Xu, T. Zhou, Y. Huo,J. Mol. Struct.(THEOCHEM).900(2009) 33.
- [20] R. Arenal, A.C. Ferrari, S. Reich, L. Wirtz, J.Y.

- Mevellec, S. Lefrant, A. Rubio, A. Loiseau, Nano. Lett. 6(2006)1812.
- [21] X. Pan, Q. X. Cai, W. L. Chen, G.L. Zhuang, X.N. Li, J. G. Wang, Comp. Mat.Sci. 67(2013)174.
- [22] E.M. Fernandez, R.I. Eglitis, G. Borstel, L.C. Balbas, Comp. Mat.Sci. 39(2007)587.
- [23] R. L. Liang, Y. Zhang, J. M. Zhang, Appl. Surf. Sci. 257(2010) 282.
- [24] H. R. Liu, H. Xiang, X. G. Gong, J. Chem. Phys. 135(2011) 214702.
- [25] A. Ricca, J. A. Drocco, Chem. Phys. Let. 362(2002) 217.
- [26] M. Barberio, P. Barone, A. Bonanno, F. Xu, Super. Microstr. 46(2009) 365.
- [27] F. Xu, M. Minniti, C. Giallombardo, A. Cupolillo, P. Barone, A. Oliva, L. Papagno, Surf. Sci. 601(2007) 2819.
- [28] A. B. Silva-Tapia, X. Garcia-Carmona, L. R. Radovi, CARBON ,50(2012) 1152.
- [29] P. Giannozzi, R. Car, G. Scoles, J. Chem. Phys. 118(2003) 1003.
- [30] Y. Chen, C. L. Hu, J. Q. Li, G. X. Jia, Y. F. Zhang, Chem. Phys. Let. 449(2007) 149.
- [31] A. Montoya, J. O. Gil, F. Mondragón, T. N. Truong, Fuel. Chem. Div. Prep. 47(2002) 424.
- [33] T. Baei, A. Ahmadi Peyghan, Z. Bagheri, Chin. Chem. Let. 23(2012) 965.
- [34] Y.L. Wang, S. Tan, J. Wang, Z.J. Tan, Q.X. Wu, Z. Jiao, M.H. Wu, Chin. Chem. Lett. 22(2011) 603.
- [34] R. Khorrampour, M.D. Esrafil, N.L. Hadipour, Physica E, 41(2009)1373.
- [35] M. Rezaei-Sameti, Physica E. 44(2012) 1770.
- [36] M. Rezaei-Sameti, Physica B. 407(2012) 3717.
- [37] M. Rezaei-Sameti, Physica B. 407(2012) 22.
- [38] M. Rezaei-Sameti, Quant. Matt., 2(2013) 1.
- [39] C. Lee, W. Yang, R. G. Parr, (1988). Phys. Rev. B. 37785.
- [40] M.J. Frisch, G.W. Trucks, H.B. Schlegel, G.E. Scuseria, M.A. Robb, J. Cheeseman, V.G. Zakrzewski, J.A. Montgomery, R.E. Stratmann, J.C. Burant, S. Dapprich, M. Millam, J.M. Daniels, A.D. Kudin, K.N. Strain, M.C. Farkas, O. Tomasi, J. Barone, V. Cossi Cammi, R. Mennucci, B. Pomelli, C. Adamo, C. Clifford, S. Ochterski, J. Petersson, G.A. Ayala, P.Y. Cui, K. Morokuma, Q. Salvador, P. Dannenberg, J.J. Malick, D.K. Rabuck, A.D. Raghavachari, K. Foresman, J.B. Cioslowski, J.J.V. Ortiz, B.B. Stefanov, G. Liu, A. Liashenko, P. Piskorz, I. Komaromi, R. Gomperts, R.L. Martin, D.J. Fox, T. Keith, M.A. Al-Laham, C.Y. Peng, A. Nanayakkara, C. Gonzalez, M. Challacombe, P.M.W. Gill, B. Johnson, W. Chen, M.W. Wong, J.L. Andres, C. Gonzalez, M. Head-Gordon, E.S. Replogle, J.A. Pople, GAUSSIAN 98.
- [41] R. Ditchfield, W.J. Hehre, J. A. Pople, J. Chem. Phys. 54(1972) 724 .
- [42] M. T. Baei, M. Moghimi, P. Torabi, A. VarastehMoradi, Comput. Theo1. Chem. 972 (2011)14.
- [43] P. K. Chattaraj, U. Sarkar, D. R. Roy, Chem. Rev. 106(2006) 2065.
- [44] K. K. Hazarika, N. C. Baruah, R. C. Deka, Struct. Chem. 20(2009). 1079.
- [45] R. G. Parr, L. Szentpaly, S. Liu, J. Am. Chem. Soc. 121(1999) 1922.